



University of Groningen

## Real-time NO<sub>2</sub> detection at ppb level with ZnO field-effect transistors

Andringa, Anne-Marije; Smits, Edsger C. P.; Klootwijk, Johan H.; de Leeuw, Dago M.

*Published in:*

Sensors and actuators b-Chemical

*DOI:*

[10.1016/j.snb.2013.01.026](https://doi.org/10.1016/j.snb.2013.01.026)

**IMPORTANT NOTE:** You are advised to consult the publisher's version (publisher's PDF) if you wish to cite from it. Please check the document version below.

*Document Version*

Publisher's PDF, also known as Version of record

*Publication date:*

2013

[Link to publication in University of Groningen/UMCG research database](#)

*Citation for published version (APA):*

Andringa, A-M., Smits, E. C. P., Klootwijk, J. H., & de Leeuw, D. M. (2013). Real-time NO<sub>2</sub> detection at ppb level with ZnO field-effect transistors. *Sensors and actuators b-Chemical*, 181(11), 668-673.  
<https://doi.org/10.1016/j.snb.2013.01.026>

### Copyright

Other than for strictly personal use, it is not permitted to download or to forward/distribute the text or part of it without the consent of the author(s) and/or copyright holder(s), unless the work is under an open content license (like Creative Commons).

### Take-down policy

If you believe that this document breaches copyright please contact us providing details, and we will remove access to the work immediately and investigate your claim.

Downloaded from the University of Groningen/UMCG research database (Pure): <http://www.rug.nl/research/portal>. For technical reasons the number of authors shown on this cover page is limited to 10 maximum.



# Real-time NO<sub>2</sub> detection at ppb level with ZnO field-effect transistors

Anne-Marije Andringa<sup>a,b</sup>, Edsger C.P. Smits<sup>c</sup>, Johan H. Klotwijk<sup>b</sup>, Dago M. de Leeuw<sup>a,d,\*</sup>

<sup>a</sup> University of Groningen, Zernike Institute for Advanced Materials, Nijenborgh 4, 9747 AG Groningen, The Netherlands

<sup>b</sup> Philips Research Laboratories, High Tech Campus 4, 5656 AE Eindhoven, The Netherlands

<sup>c</sup> Holst Centre, High Tech Campus 31, 5656 AE Eindhoven, The Netherlands

<sup>d</sup> Max Planck Institute for Polymer Research, Ackermannweg 10, D-55128 Mainz, Germany

## ARTICLE INFO

### Article history:

Received 29 August 2012

Received in revised form

26 November 2012

Accepted 8 January 2013

Available online xxx

### Keywords:

NO<sub>2</sub> sensors

Field-effect transistor

Electron trapping

Threshold voltage shift

Stretched-exponential

Real-time sensor

Dynamic read out

## ABSTRACT

We present a functional real-time NO<sub>2</sub> sensor based on a ZnO field-effect transistor. The dynamic response of the sensor is calculated using a phenomenological charge trapping model, using only experimentally determined parameters. This analytical model is implemented in the sensor protocol to create a hardware demonstrator sensor. We show that the partial NO<sub>2</sub> pressure in ambient air can be monitored in real-time for concentrations as low as 40 ppb. The response is verified by simultaneously measuring the NO<sub>2</sub> content with a calibrated reference sensor. A perfect agreement between the measured and reference data is obtained, which validates the methodology. The sensor is fabricated using standard IC technology, which can easily be miniaturized and used in handheld applications.

© 2013 Elsevier B.V. All rights reserved.

## 1. Introduction

Nitrogen dioxide, NO<sub>2</sub>, is a dangerous air pollutant affecting human health and the environment. The gas is released during the combustion of fossil fuels and plays a major role in the formation of ozone, acid rain and photochemical smog. The huge amounts of NO<sub>2</sub> released into the atmosphere everyday can cause fatal problems not only to human beings but also to animals and plants, both aquatic and terrestrial [1]. Current scientific evidences relate short-term exposure to NO<sub>2</sub> gas to adverse respiratory effects including airway inflammation in healthy people and increased respiratory problems in asthma patients, while long-term exposure is correlated to pulmonary edema and death. For real-time monitoring and controlling air quality, sensitive, calibrated and reliable NO<sub>2</sub> sensors are required.

The most common NO<sub>2</sub> sensors are chemiresistors based on semiconducting metal oxides such as SnO<sub>2</sub>, WO<sub>3</sub>, or ZnO [2–4]. Thick porous oxide layers with high specific surface area are used. The gas diffuses into the oxide layer and modulates the grain boundary resistances by transfer of charge carriers from the semiconductor to the adsorbed surface species. To optimize the sensing

characteristics the mixed metal oxides are being doped with trace amounts of e.g. noble metals for their catalytic properties [5]. An overview of the state-of-the-art performance of NO<sub>2</sub> sensing with chemiresistors based on metal oxides has recently been reported [6]. The operating temperature is typically around 200 °C, the response time is around 1 min, the detection range in the order of 1–100 ppm NO<sub>2</sub>, and the gas response as relative resistance change is around 10–100% per ppm NO<sub>2</sub>. Issues are long term stability, reliability and cross sensitivity for other gases especially oxygen, although the lack of selectivity can be overcome by using differential reading of multi sensor arrays.

Field-effect transistors (FETs) have emerged as an alternative NO<sub>2</sub> sensing technology [6–8]. A field-effect transistor is a three terminal device where an additional electrode modulates the charge carrier density in the semiconductor. The current through the semiconductor can be altered over orders of magnitude. Hence, a sensor based on a FET is intrinsically more sensitive. Experimentally it has been shown that the electrical transport does not change when the transistor is exposed to NO<sub>2</sub>. However, the transport changes in an NO<sub>2</sub> ambient when a continuous gate bias is applied. This change can be monitored by shortly interrupting the continuous gate bias and measuring a transfer curve. As shown schematically in Fig. 1a the transfer curve then shifts with time to the applied gate bias. The shape remains the same. The only change is the threshold voltage, here empirically taken as the onset of current modulation. The mechanism is due to gate bias controlled charge

\* Corresponding author at: Max Planck Institute for Polymer Research, Ackermannweg 10, D-55128 Mainz, Germany.

E-mail address: [deleeuw@mpip-mainz.mpg.de](mailto:deleeuw@mpip-mainz.mpg.de) (D.M. de Leeuw).

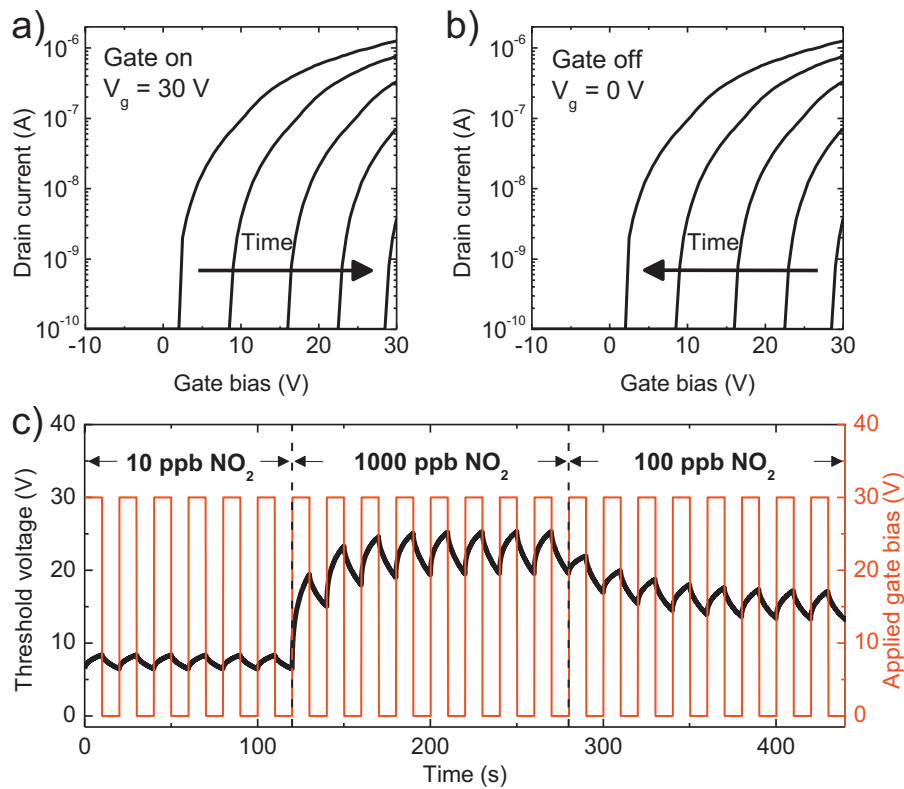


**Fig. 1.**  $\text{NO}_2$  sensing principle with a field-effect transistor. (a) Schematically depicted transfer curves of a field-effect transistor in an  $\text{NO}_2$  ambient upon charging. When a continuous gate bias of 30 V is applied, the transfer curve shifts with time, as indicated by the arrow. The threshold voltage starts at 0 V and saturates at the applied gate bias of 30 V. (b) Recovery: when a 0 V gate bias is applied, the threshold voltage shifts back with time to its original value. The temperature is set to obtain comparable time constants for trapping and recovery. (c) Analytically calculated threshold voltage response as a function of time under intermittently applying a gate bias. The applied gate bias is indicated in red. The threshold voltage shifts up and downwards under charging and recovery. The dynamic equilibrium value is reached that depends on the partial  $\text{NO}_2$  pressure. The  $\text{NO}_2$  content is varied with time as indicated. (For interpretation of the references to color in the artwork, the reader is referred to the web version of the article.)

trapping of electrons at the gate dielectric ZnO interface [9,10]. When the gate bias is turned off, the trapped electrons are thermally released and the threshold voltage recovers to its original value as schematically depicted in Fig. 1b. The time constants for charging and recovery depend on temperature and partial  $\text{NO}_2$  pressure. By intermittently turning the gate bias on and off, the threshold voltage shifts up and down and a dynamic equilibrium of the threshold voltage is reached. The gate bias pulse sequence and temperature can be chosen in such a way that the dynamic equilibrium of the threshold voltage depends on the partial  $\text{NO}_2$  pressure (Fig. 1c). The field-effect transistor then functions as a dynamic real-time sensor.

Previously, we have modeled the temporal behavior of the threshold voltage to set the operating temperature and cycle time to obtain a reversible sensor [10]. The model uses as input the threshold voltage dynamics as a function of temperature and  $\text{NO}_2$  pressure as measured for both charging and recovery. The response of the transistor can then be calculated with experimentally determined parameters, without the use of any additional fit parameters. Here we implement the phenomenological model into a hardware demonstrator sensor. We show that the partial  $\text{NO}_2$  pressure in air can be monitored in real time. Concentrations as low as 40 ppb have been detected. The measurements are verified by comparing the sensor response with a calibrated commercial  $\text{NO}_2$  detector.

## 2. Sensor fabrication

### 2.1. ZnO field-effect transistor and characterization

The fabrication and characterization of unipolar  $n$ -type ZnO field-effect transistors have been described in detail in Ref. [9]. Briefly, transistor test structures were fabricated on heavily doped

$n$ -type Si wafers, acting as common gate electrode, with a 200 nm thermally oxidized  $\text{SiO}_2$  layer as gate dielectric. Gold source and drain electrodes were defined by conventional photolithography, resulting in interdigitated transistors with a channel length of 10  $\mu\text{m}$  and a width of 10,000  $\mu\text{m}$ . A photograph of a 150 mm wafer containing multiple test substrates together with a detailed photograph of a single substrate and a schematic of the transistor cross section are depicted in Fig. 2. The ZnO was applied using spray pyrolysis in ambient atmosphere [11]. A solution of zinc acetate in methanol was nebulized and deposited on top of a single transistor substrate, heated at 400  $^\circ\text{C}$ . XRD and AFM measurements showed that the 10 nm thick ZnO layers exhibited a microcrystalline morphology. To reduce the surface conductivity of the ZnO layer, a self-assembled-monolayer (SAM) of  $n$ -octadecyl phosphonic acid

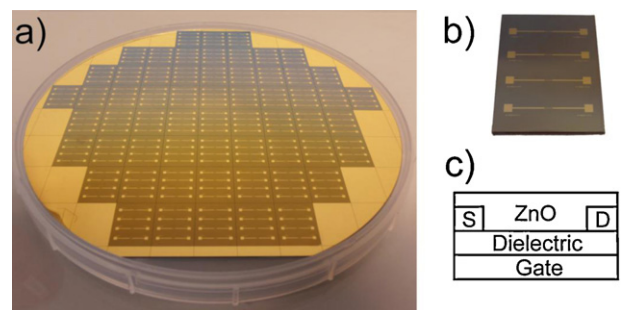


**Fig. 2.** (a) Photograph of a 150 mm monitor wafer containing multiple test substrates. (b) Photograph of a single test substrate containing four interdigitated Au transistor structures, with a channel length and width of 10 and 10,000  $\mu\text{m}$ , respectively. (c) Schematic cross section of the transistor.

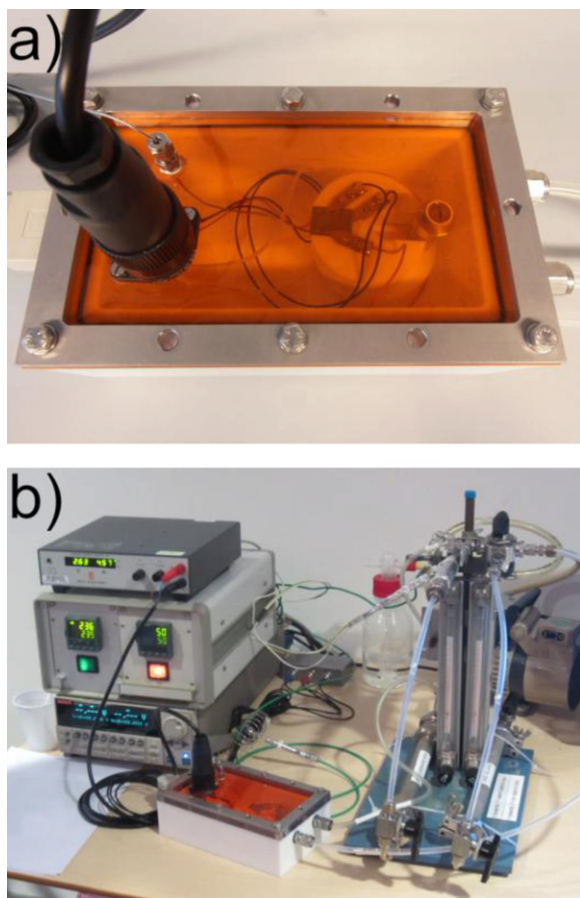


**Fig. 3.** Sensor cell and system. (a) Photograph of the Teflon sensor cell containing a ZnO field-effect transistor mounted on a heater. For demonstration purposes a large box was used. The lid of the flow cell was covered with orange foil that filters UV light. (b) Photograph of the complete sensor system containing the sensor cell, Teflon tubings, additional flow meters, NO<sub>2</sub> permeation tube, molsieves moisture filters, vacuum pump and peripheral electronics.

was applied from a 3 mM ethanol solution. The SAM was tested to have no effect on the sensitivity toward NO<sub>2</sub>. The passivated ZnO transistors had a field-effect mobility of 0.1–2 cm<sup>2</sup> V<sup>−1</sup> s<sup>−1</sup> and showed negligible hysteresis and high stability under gate bias stress in inert atmosphere.

## 2.2. Sensor cell and system

The sensor cell was fabricated from Teflon and equipped with feed-throughs for the electrical source, drain and gate contacts. For demonstration purposes a large box of 0.4 L was used. A photograph is presented in Fig. 3a. The transistor was placed on to a ceramic plateau, fitting around a UHV Substrate Heater (HeatWave Labs, Inc.) and contacted. The temperature of the heater, electrically insulated from the transistor substrate by a locally thin ceramic sheet, was regulated using a Eurotherm 2416 controller and a Delta power supply. To maintain visibility of the sensor but to prevent UV irradiation from distorting the measurement, the polycarbonate lid of the flow cell was covered with an orange foil that filters UV light.

A block diagram of the gas flow system is depicted in Fig. 4. Air flow was achieved by using a diaphragm vacuum pump. Teflon tubings were used. Ambient air was dried using molsieves (Type 3A, 8–12 mesh beads, Janssen Chimica). No other precautions were taken. The humidity of the exhausted air was measured to be 40 ppm, 0.2% of the original humidity. As NO<sub>2</sub> source, a permeation tube was chosen with a calibrated emission rate of 369 ng/min at

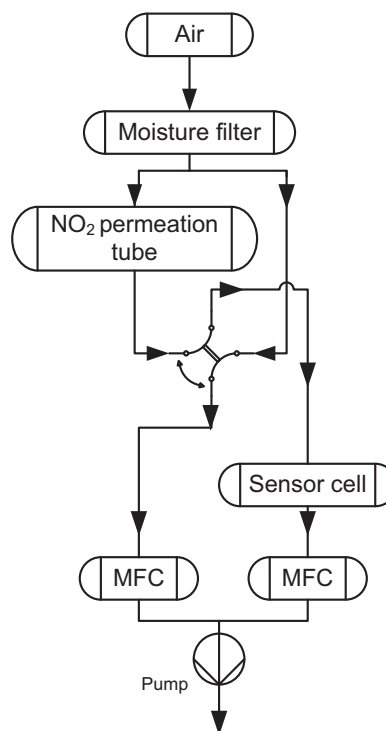


**Fig. 4.** Block diagram of the gas flow system. An air flow was achieved by using a diaphragm vacuum pump. Ambient air was dried with molsieves. As an NO<sub>2</sub> source a permeation tube was used. A 4-port 2-way valve was applied to switch the NO<sub>2</sub> flow from the sensor cell to the bypass, while ensuring continuous flow over the permeation tube. With two mass flow controllers (MFC) the flow speeds were regulated through the sensor cell and the bypass.

45 °C and 200 sccm (Kin-Tek). The temperature of the permeation tube was regulated with a Eurotherm 2216e controller. A 4-port 2-way valve was applied to switch the NO<sub>2</sub> flow from the sensor cell to the bypass, while ensuring continuous flow over the permeation tube. Two mass flow controllers were used to regulate the flow speeds through the sensor cell and the bypass. For calibrated measurements, the exhausted flow from the sensor cell was redirected to a commercial reference sensor based on chemiluminescence, an Eco Physics CLD 88p NO analyser. A gas converter (series CG, M&C TechGroup) was used to convert NO<sub>2</sub> catalytically to NO at 330 °C with a carbon molybdenum mixture. Electrical measurements were carried out using a Keithley 2602 System SourceMeter controlled by an in-house developed Labview program as described in the next section. A photograph of the complete sensor system is presented in Fig. 3b.

## 3. Methodology and implementation

To set the operating temperature, the pulse time and duty cycle for a reversible, calibrated sensor we first have modeled the temporal behavior of the threshold voltage as reported in Ref [10]. To this end, charging and recovery measurements have been performed on ZnO field-effect transistors as a function of temperature and NO<sub>2</sub> pressure as described previously [10]. For a given NO<sub>2</sub> content the threshold voltage as a function of time during charging with a continuous applied gate bias at various temperatures follows a stretched-exponential time dependence:

$$\Delta V_{th}(t) = V_0 \left\{ 1 - \exp \left[ - \left( \frac{t}{\tau} \right)^\beta \right] \right\} \quad (1)$$

where  $\tau$  is a relaxation time, the dispersion parameter  $\beta$  equals  $T/T_0$ , where  $T_0$  is a characteristic temperature, and  $V_0 = V_G - V_{th0}$ , where



$V_G$  is the applied gate bias and  $V_{th0}$  is the threshold voltage at the start of the experiment. The relaxation time is thermally activated as:

$$\tau = \nu^{-1} \exp\left(\frac{E_a}{k_B T}\right) \quad (2)$$

where  $E_a$  is an activation energy,  $k_B$  the Boltzmann constant, and  $\nu$  is the so-called attempt-to-escape frequency. For a given ZnO transistor the extracted parameters  $\nu$ ,  $T_0$  and  $E_a$  are fixed. Upon varying the  $\text{NO}_2$  pressure they do not change. Only the relaxation time depends on the  $\text{NO}_2$  pressure as:

$$\tau \approx \frac{1}{p_{\text{NO}_2}} \quad (3)$$

To quantitatively describe the  $\text{NO}_2$  dependence we therefore normalize Eq. (2) as:

$$\tau = \frac{p_{\text{NO}_2}^*}{p_{\text{NO}_2}} \nu^{-1} \exp\left(\frac{E_a}{k_B T}\right) \quad (4)$$

where the normalization constant  $p_{\text{NO}_2}^*$  is the partial pressure at which the frequency factor  $\nu$  has been determined. Hence the complete charging dynamics, viz. the time, bias, temperature and  $\text{NO}_2$  dependence can be described by only three parameters,  $\nu$ ,  $T_0$  and  $E_a$ , that are constant for a given transistor and a normalization factor for the  $\text{NO}_2$  concentration. The extracted values for the present transistor are 11 Hz, 960 K and 0.1 eV, respectively. The underlying physics of the charge trapping process has been presented in Ref. [10]. The parameters can be extracted from a single measurement set and then be used to quantitatively predict the complete charging dynamics.

Similarly the recovery can be described by a stretched-exponential time dependence with a thermally activated relaxation time, Eqs. (1) and (2). The relaxation time for recovery is independent of  $\text{NO}_2$  content. Hence, the recovery can quantitatively be described with three parameters,  $\nu$ ,  $T_0$  and  $E_a$ , that are constant for a given transistor. For recovery the extracted values are  $10^{11}$  Hz, 750 K and 1.2 eV, respectively. The underlying physics of the recovery process has been presented in Ref. [10].

To operate the  $\text{NO}_2$  sensor we turn the gate intermittently on and off. The gate bias as a function of time is depicted as the red block diagram in Fig. 1c. The  $\text{NO}_2$  concentration is varied with time from 10 ppb for the first 120 s, then 1000 ppb for the next 160 s and finally 100 ppb for 160 s. The black curve represents the threshold voltage as a function of time, calculated using Eqs. (1) and (2) or (4) for recovery or charging, respectively. When a gate bias is applied the transistor is charged and the threshold voltage shifts. When the transistor is turned off, the transistor recovers. By pulsing the gate, the threshold voltage oscillates between a maximum voltage after charging and a minimum voltage after recovery. After a number of cycles, equilibrium is reached, in which the threshold voltage at the end of the charging pulse corresponds to the partial  $\text{NO}_2$  pressure.

The flow chart to determine the  $\text{NO}_2$  partial pressure from the dynamic electrical measurement of the sensor is presented in Fig. 5. First a look up table is created. The three parameters describing the charging dynamics and the three parameters describing the recovery are used as input. Then the gate bias, the measurement protocol and temperature are set. For a given  $\text{NO}_2$  pressure the threshold voltage is calculated as a function of time using Eqs. (1) and (2) or (4) for recovery or charging, respectively. In the calculation, a correction for probing the threshold voltage is implemented by taking into account the average charging and recovery time of the transfer curve measurement. The calculations are continued until convergence is reached, indicating that the dynamic equilibrium has been obtained. The minimum and maximum extracted voltages are stored together with the set  $\text{NO}_2$  pressure. The look

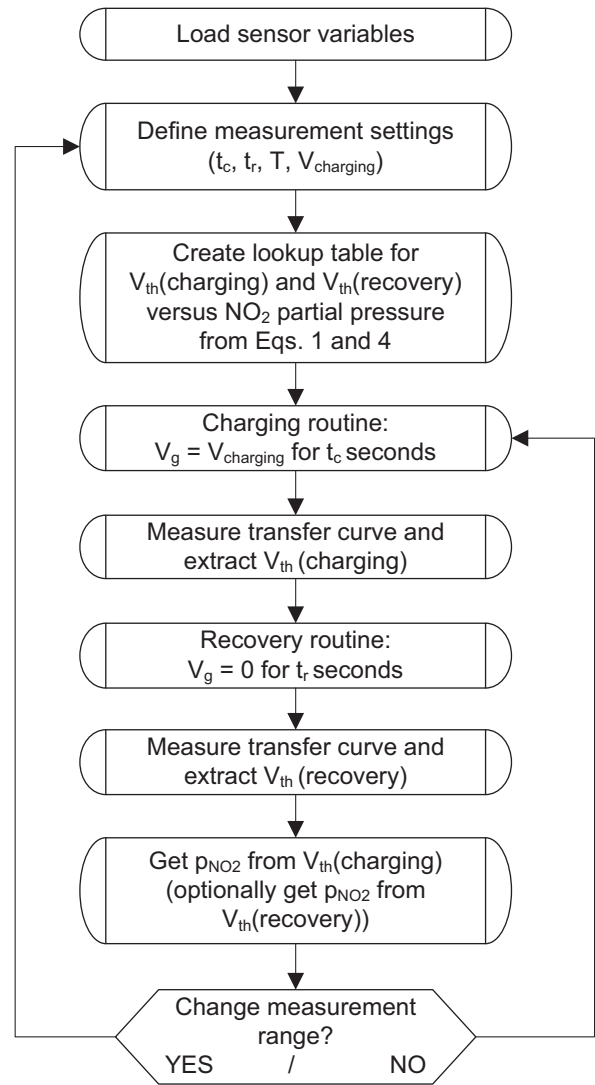


Fig. 5. Flow chart to determine the  $\text{NO}_2$  partial pressure from the electrical measurement of the sensor.

up table is completed for the relevant  $\text{NO}_2$  pressures and used as calibration curve.

The gate bias protocol and temperature chosen in the model are applied to the transistor. As measurement protocol we used 10 s gate bias pulse at 30 V for charging and 10 s at zero gate bias for recovery. The temperature was set at 200 °C. Based on the activation energies of charge trapping and release, experimentally determined in Ref. [10], the sensor is reversible at this temperature. The threshold voltage is experimentally extracted at the end of each charging and recovery pulse. To this end a transfer curve is recorded, by measuring the source-drain current with increasing gate bias at a low drain bias of 2 V. To reduce charge trapping during the probing of the threshold voltage, the transfer curves were measured using a short integration time and a compliance stop. The compliance stop was chosen at 100 nA, one decade above the noise of the off current. The threshold voltage is extracted from the final gate bias by subtracting a fixed offset of 2 V. This offset was experimentally determined. The threshold voltage is translated into  $\text{NO}_2$  concentrations using the lookup table. The discretisation of the threshold voltage sets the  $\text{NO}_2$  concentration resolution. Finally, in the case that the transistor is sensitive to conventional gate bias stress, due to e.g. high back ground humidity, the look up table has to be adapted.

#### 4. Sensor verification

To perform dynamic measurements a transistor was mounted in the sensor cell and the heater was set at 200 °C. The vacuum pump was turned on and the system was flushed with air for one hour. The measurement protocol was started and the permeation tube was heated to deliver a certain amount of NO<sub>2</sub>. The signal from the sensor was processed as described above in Section 3 and recorded. The flow was switched intermittently from air with to air without NO<sub>2</sub>. The NO<sub>2</sub> content was varied by adjusting the temperature of the permeation tube. The dynamic sensor response, the NO<sub>2</sub> concentration as a function of time, is presented in Fig. 6 as the black curve.

The discretisation of the determined threshold voltage was set at 0.1 V which yields a resolution in NO<sub>2</sub> concentration of about 20 ppb. The lowest stable concentration achieved, set by the minimum quantity the permeation tube can deliver, was 40 ppb. The base line is about 10 ppb. This background is due to degassing of the Teflon walls of the sensor cell. The sensor is capable to detect these minimal changes in concentrations. The sensor was tested up to an NO<sub>2</sub> level of 1 ppm. Above 1 ppm, the threshold voltage is almost at the applied gate bias and the concentration can no longer be resolved. When a higher concentration range is desired, this saturation can be addressed by reducing the stress time or by increasing the temperature.

The response time of the sensor at 200 °C lies between tens to hundreds of seconds. A new value of the threshold voltage is recorded every 22 s and compared to the calibration curve calculated in equilibrium. When the concentration in the system has changed, a new equilibrium has to be obtained by performing multiple measurement cycles. The equilibrium is reached faster at higher temperatures and higher NO<sub>2</sub> concentrations. The response time can be further optimized by adjusting the measurement protocol. However, there will be an inherent trade off between sensitivity and response time. In addition, the enormous dead volume of the current sensor cell prevents fast intermixing and limits the time resolution to around 100 s.

To verify the sensor response we simultaneously measured the NO<sub>2</sub> content with the EcoPhysics NO sensor system. The recorded response is presented in Fig. 6 as the red curve. A good agreement between the measured and reference data is obtained, which validates our methodology. Only a minor drift in the NO<sub>2</sub> concentration measured by the ZnO FET sensor was observed. The nature of the

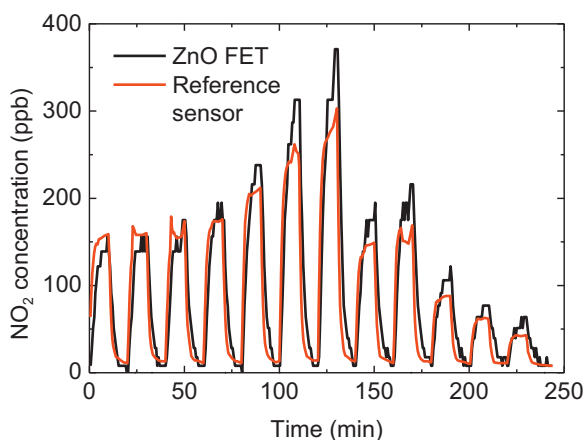


**Fig. 6.** Sensor verification. The ZnO field-effect transistor sensor was heated, turned on and equilibrated. Then the NO<sub>2</sub> concentration was set by adjusting the temperature of the permeation tube. The flow was switched by the 4-port 2-way valve between sensor and bypass. The measured NO<sub>2</sub> concentration as a function of time is presented by the black line. The red line represents the NO<sub>2</sub> content as simultaneously measured with a calibrated commercial reference sensor.

drift is unclear, possible reasons are slight variations in temperature or influence of the residual 40 ppm water.

The EcoPhysics NO sensor is a compact expensive stand-alone system being used for environmental monitoring, industrial applications such as waste incineration, and exhaled breath analysis in hospitals. The price prohibits point of care use. Here we have shown that a similar performance can be obtained with a single field-effect transistor as NO<sub>2</sub> transducer. The transistor is fabricated using standard IC technology, which can easily be miniaturized and used in a variety of handheld applications. The detection is not optical but only electrical. The implementation of the transducer can therefore lead to a major cost reduction of an NO<sub>2</sub> detection system.

The present sensor is sensitive to water: operating the sensor in wet air causes instability observed as a baseline drift. The absorption of water onto a gate dielectric such as SiO<sub>2</sub> in transistors causes threshold voltage shifts. Surface passivation of silanol groups by organic primers (e.g. HMDS or OTS) have been shown to strongly reduce these instabilities [12]. Optimization of the gate dielectric of the ZnO sensor might solve this problem, but experiments have not been attempted. Instead we used molsieves to dry the ambient air. The water content was measured to be at most 40 ppm. This procedure is sufficient to yield a reliable sensor. Regeneration of the molsieves is needed after one week of full operation. The ZnO transistor was stable in NO. The sensor in combination with the developed measurement protocol did also not show baseline drifts in compressed dry air, indicating that the sensor is insensitive to oxygen. Although the sensor dynamics and extracted parameters were determined from measurements performed in nitrogen [10] they could be successfully used to determine the NO<sub>2</sub> concentration in the ambient air dried by the molsieves. The shelf life of the sensors in ambient was found to be over a year and under dry conditions the sensor has been operated for a multiple days without any drop in performance.

#### 5. Summary and conclusion

We have presented a functional real-time NO<sub>2</sub> sensor based on a ZnO field-effect transistor. The dynamic response of the sensor is calculated using a phenomenological charge trapping model, using only experimentally determined parameters. The parameters are constant for a given transistor and have been determined previously. The analytical model is implemented in the sensor protocol to create a hardware demonstrator sensor. A sensor has been fabricated and tested. The NO<sub>2</sub> concentration is measured in real time. The response is verified by simultaneously measuring the NO<sub>2</sub> content with a calibrated reference sensor. The perfect agreement obtained validates the sensor and methodology.

The sensor is capable of detecting concentrations as low as 40 ppb. The sensor functions up to an NO<sub>2</sub> level of 1 ppm. When a different concentration range is desired, the detection protocol can be adapted. The sensor operates in ambient air. Apart from drying with molsieves, no further precautions were taken to filter the air, showing that the fabricated sensor is selective for NO<sub>2</sub>. The real-time detection of low concentrations of NO<sub>2</sub> down to the ppb level sets a precedent for sensing with field-effect transistors.

#### Acknowledgements

We gratefully acknowledge technical assistance from H. Verberne, T.C.T. Geuns and P.V.E. Krusemann at MiPlaza, Eindhoven, and from B. Giesbers and M. Spijkman at Philips Research and financial support from the Zernike Institute for Advanced Materials, the Netherlands Organization for Scientific Research (NWO, Vidi grant, 700.57.425) and from the EC (project ONE-P no. 212311).

## References

- [1] Environmental Protection Agency (EPA), Air Pollution, 2012. <http://www.epa.gov/air/nitrogenoxides/> (accessed 18.07.12).
- [2] N. Barsan, D. Koziej, U. Weimar, Metal oxide-based gas sensor research: how to? *Sensors and Actuators B: Chemical* 121 (2007) 18–35.
- [3] N. Barsan, U. Weimar, Conduction model of metal oxide gas sensors, *Journal of Electroceramics* 7 (2001) 143–167.
- [4] T. Inoue, K. Ohtsuka, Y. Yoshida, Y. Matsuura, Y. Kajiyama, Metal oxide semiconductor NO<sub>2</sub> sensor, *Sensors and Actuators B: Chemical* 25 (1995) 388–391.
- [5] P. Ivanov, E. Llobet, F. Blanco, A. Vergara, X. Vilanova, I. Gracia, C. Cane, X. Correig, On the effects of the materials and the noble metal additives to NO<sub>2</sub> detection, *Sensors and Actuators B: Chemical* 118 (2006) 311–317.
- [6] A. Afzal, N. Cioffi, L. Sabbatini, L. Torsi, NO<sub>x</sub> sensors based on semiconducting metal oxide nanostructures: progress and perspectives, *Sensors and Actuators B: Chemical* 171–172 (2012) 25–42.
- [7] A. Das, R. Dost, T. Richardson, M. Grell, J.J. Morrison, M.L. Turner, A nitrogen dioxide sensor based on an organic transistor constructed from amorphous semiconducting polymers, *Advanced Materials* 19 (2007) 4018–4023.
- [8] G. Barillaro, A. Diligenti, A. Nannini, L.M. Strambini, E. Comini, G. Sberveglieri, Low-concentration NO<sub>2</sub> detection with an adsorption porous silicon FET, *Ieee Sensors Journal* 6 (2006) 19–23.
- [9] A. Andringa, J.R. Meijboom, E.C.P. Smits, S.G.J. Mathijssen, P.W.M. Blom, D.M. de Leeuw, Gate-bias controlled charge trapping as a mechanism for NO<sub>2</sub> detection with field-effect transistors, *Advanced Functional Materials* 21 (2011) 100–107.
- [10] A. Andringa, N. Vlietstra, E.C.P. Smits, M. Spijkman, H.L. Gomes, J.H. Klootwijk, P.W.M. Blom, D.M. de Leeuw, Dynamics of charge carrier trapping in NO<sub>2</sub> sensors based on ZnO field-effect transistors, *Sensors and Actuators B: Chemical* 171–172 (2012) 1172–1179.
- [11] A. Bashir, P.H. Wobkenberg, J. Smith, J.M. Ball, G. Adamopoulos, D.D.C. Bradley, T.D. Anthopoulos, High-performance zinc oxide transistors and circuits fabricated by spray pyrolysis in ambient atmosphere, *Advanced Materials* 21 (2009) 2226–2231.
- [12] S.G.J. Mathijssen, M. Kemerink, A. Sharma, M. Coelle, P.A. Bobbert, R.A.J. Janssen, D.M. de Leeuw, Charge trapping at the dielectric of organic transistors visualized in real time and space, *Advanced Materials* 20 (2008) 975–979.